Volume 1, No.1, March – April 2012
International Journal of Advanced Trends in Computer Science and Engineering
Available Online at www.warse.ijatcse.current

CFD Analysis of Supersonic combustion using Diamond shaped Strut Injector with standard K-Є Non-premixed Turbulence model

K.M.Pandey, Professor, Department of Mechanical Engineering,N.I.T Silchar, India,
kmpandey2001@yahoo.com
Sukanta Roga, M.Tech Student, Department of Mechanical Engineering, N.I.T Silchar,India,
sukanta.me42@gmail.com
A.P.Singh, Lecturer,Department of Mechanical Engineering, N.I.T Silchar, India,
hello2apsingh@gmail.com

ABSTRACT

In this paper the supersonic combustion of hydrogen using strut injector along with two-dimensional turbulent non-premixed combustion model. The present work is based on the standard k- ε which has been used for modeling the turbulence and single step finite rate chemistry. In this process, a PDF (Probability Density Function) approach is created and this method needs solution to a high dimensional PDF transport equation. After designing the model in GAMBIT, it is exported to FLEUNT software for analysis of combustion process with air inlet at Mach number 2 and hydrogen as the fuel with inlet Mach number 1. As the combustion of hydrogen fuel is injected from the strut injector, it is successfully used to model the turbulent reacting flow field. It is observed from the present work that, the maximum temperature occurred in the recirculation areas which is produced due to shock wave-expansion and the fuel jet losses concentration and after passing successively through such areas, temperature decreased slightly along the axis. From the maximum mass fraction of OH, it is observed that there is very little amount of OH around 0.00233 were found out after combustion. By providing strut injector, expansion wave is created which cause the proper mixing between the fuels and air which results in complete combustion.

Keywords: CFD, Combustion, Diamond-shaped Strut Injector Hydrogen Fuel, Non-premixed Combustion, Scramjet, Standard K-ε Turbulence Model, Steady State, Supersonic Combustion

1. INTRODUCTION

Propulsion concepts such as the supersonic combustion ramjet (scramjet) and the shock-induced combustion ramjet (scramjet) utilize oxygen freely available in the atmosphere and thereby substantially reduce the weight penalty of on-board oxidizer tank used in rocket based systems. In the case of a hypersonic air-breather the challenge is increased due to the requirement of supersonic combustion. Flow velocities through the combustor on the order of thousands of meters per second provide the fuel and air with only a brief time to adequately combine. Contemporary mixing augmentation methods to address this issue have focused on fuel injection devices which promote axial vortices to enhance the mixing process.

A scramjet engine is well known as hypersonic air-breathing engine in which heat release due to combustion process occurs in the supersonic flow relative to the engine. Therefore, the flow velocity throughout the scramjet remains supersonic and thereby it does not require mechanical chocking system [1]. Scramjet is an signifier for Supersonic Combustion Ramjet which is a type of jet engine aimed to operate in the high velocity regime usually it is related with rockets. Both are designed to be used for supersonic flight; however a Scramjet allows the flow through the engine to remain supersonic, whereas in a Ramjet the flow is slowed to subsonic levels before it enters the combustor which is the main difference between Scramjet and the Ramjet. Figure1 shows a basic generic Scramjet design. It works by injecting fuel into a flow of supersonic air. The air is at sufficiently high temperature and pressure for the fuel to combust and the resulting mixture is discharged from the engine at a higher pressure. The Scramjet engine is composed of four main sections: the inlet, isolator, combustor and exhaust [2].

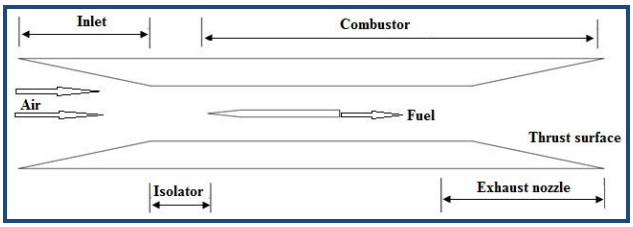

Figure 1 : Generic Scramjet engine

K.M.Pandey, T.Sivasakthivel and S.K. Reddy K.K [3][4] describe that there are many types of Fuel Injectors for Scramjet Engines. The fuel that is used by scramjets is usually either a liquid or a gas. The fuel and air need to be mixed about stoichiometric proportions for efficient combustion. The main problem of scramjet fuel injection is that the air flow is

quite fast which shows that, there is minimal time for the fuel to mix with the air and ignite to produce thrust which require about milliseconds. Hydrogen is the main fuel used for combustion. The main important aspect in designing scramjet engines is to enhance the mixing and thus reducing the combustor length. A number of options are available for injecting fuel and enhancing the mixing of the fuel and air in high speed flows typical of those found in a scramjet combustor i.e., strut injectors, planner injectors, parallel injectors, normal injectors, ramp injectors, cavity flame holder etc.

A modified design to Marble's injector was studied by Davis [5]. The fuel injector embodied the elements of the contoured wall fuel injector but was more modular since it could be mounted on a flush combustor wall. The study is focused on jet penetration and mixing behaviour under a variety of different operating conditions. A swept and unswept injector configuration was experimentally tested. The superior vortex generating ability of the swept configuration over the unswept was established. A concurrent experimental and numerical effort was undertaken to study Mach 1.7 helium (used to simulate hydrogen) injected into a Mach 6 airstream. Several parametric dependencies were investigated including: injector spacing, ramp geometry, boundary layer effects and injectant/free stream velocity and pressure ratios. A detailed description of flow fields and flow phenomena were presented. The work demonstrated that the induced vorticity coalesced into a counter-rotating pair of vortices promoting helium migration up into the main stream. The two main sources of vorticity, baroclinic torque and cross-streams hear, were identified and characterized. It concluded that shock-impingement produced effective mixing by deposition of baroclinic torque at the fuel air interface while cross-stream shear induced vorticity can be less effective due to vortices generated remote from the fuel air interface. Flow visualization was employed to identify salient flow features.

Haimovitch experimentally investigated six different injector-nozzle inserts to precondition the fuel flow. Mie scattering visualization revealed a minor difference in the mixing performance between the candidate injectors. More comprehensive computational results were provided by Eklund [6] who studied Mixing in the context of a reacting flow field the Navier-Stokes equations were solved with a finite-rate chemical kinetics model for H_2-air reaction together with an algebraic eddy viscosity turbulence model. A reduction of up to 25% in mixing efficiency was observed for the reacting case. Larger computational grids were employed simulating laminar and turbulent mixing. Insightful analysis of results underscored the dominant role of turbulence in the far-field, although turbulence modelling issues were not fully addressed. The injector nozzle flow was included as part of the computational domain which consisted of a remarkable 13.5 million grid nodes. J. Schumacher [7] studied the Numerical Simulation of Cantilevered Ramp Injector Flow Fields for Hyper velocity Fuel-Air Mixing Enhancement. Dudebout,R.Sislian, J.P., and Oppitz. R. [8] studied hypersonic air-breathing propulsion using shock-induced combustion ramjets using 2D geometries with planar and axisymmetric configurations, as well as external and mixed-compression configurations.

Jeung et al. [9] renewed interest on the scramjet engine has been demonstrated through the many international activities along the several Asia-Pacific countries. Here, a short review of current activities on supersonic combustion in a scramjet engine will be addressed followed by the discussions on the review of numerical simulation on supersonic combustion phenomena related with scramjet engine combustors and ram accelerator. Emphasis was put on the grid refinement, scheme, unsteadiness and phenomenological differences.

Kim et al. [10] studied the numerical investigations concerning the combustion enhancement when a cavity is used for the hydrogen fuel injection through a transverse slot nozzle into a supersonic hot air stream. Several inclined cavities with various aft wall angle, offset ratio and length are evaluated for reactive flow characteristics. The cavity effect is discussed from a viewpoint of total pressure loss and combustion efficiency. The combustor with cavity is found to enhance mixing and combustion while increasing the pressure loss, compared with the case without cavity. But it is noted that there exists an appropriate length of cavity regarding the combustion efficiency and total pressure loss.

Recent results from combustion experiments reviewed in a direct-connect supersonic combustor are presented by Mathur et al. [11]. Successful ignition and sustained combustion of gaseous ethylene have been achieved using an injector/flameholder concept with low-angle, flush-wall fuel injection upstream of a wall cavity. Two interchangeable facility nozzles (Mach 1.8 and 2.2) were used to obtain combustor inlet flow properties that simulate flight conditions between Mach 4 and 6 at a dynamic pressure of 47.9 kPa. Mainstream combustion was achieved at equivalence ratios between 0.25 and 0.75 using only a spark plug and no other external ignition aids. Delta-force levels between 667 and 1779 N were measured, with corresponding combustor pressure ratios between 3.1 and 4.0. Video records of the flame zone show an intensely active combustion zone with rapid flame spreading. One-dimensional performance analysis of the test data indicates combustion efficiency around 80%with an average combustor skin friction coefficient of 0.0028
Activities in the area of scramjet fuel-air mixing and combustion associated with the Research and Technology Organization Working Group on Technologies for Propelled Hypersonic Flight are described by Drummond et al. [12]. Work discussed in this paper has centered on the design of two basic experiments for studying the mixing and combustion of fuel and air in a scramjet. Simulations were conducted to aid in the design of these experiments. The experimental models were then constructed, and data were collected in the laboratory. Comparison of the data from a coaxial jet mixing experiment and a supersonic combustor experiment with a combustor code were then made and described. This work was

conducted by NATO to validate combustion codes currently employed in scramjet design and to aid in the development of improved turbulence and combustion models employed by the codes.

Hydrogen injection has been investigated numerically by Burtschell et al. [13] in a flow configuration caused by strong shock-boundary layer interaction named Viscous Mach Interaction (VMI). The geometry that leads to this configuration is used as a hypersonic inlet. The subsonic zone, because of boundary layer detachment, allows hydrogen to be injected along the wall of the central body where combustion processes occur along a slip line when hydrogen is mixed with the incoming air flow far from the wall of the central body. High-resolution two-dimensional numerical simulations have been initiated by Haworth et al. [14] for premixed turbulent propane-air flames propagating into regions of non-homogeneous reactant stoichiometry. Simulations include complex chemical kinetics, realistic molecular transport, and fully resolved hydrodynamics (no turbulence model).Ignition of methane/hydrogen and air streams in a supersonic mixing layer was investigated by Ju and Niioka [15] numerically with the C-I chemistry for interests in aerospace application. Attention was paid to ignition delay times and ignition processes with the addition of methane to hydrogen and the addition of hydrogen to methane involving elementary reactions. In the first case, results showed that the addition of methane to hydrogen dramatically affected the ignition time.

A novel approach to modelling the dynamics of an air-breathing combustion system is presented by Gupta et al. [16]. A steady-state model for the intake is obtained from 3D RANS simulations using the CFD Expert TM code, and a quasi-1D formulation with finite rate chemistry is used to model the combustor. First-order time-delays are introduced at the interface between different blocks to model the dynamics of the system.

Akbarzadeh and Kermani [17] studied on the performance of three different ramjet engine inlets is numerically considered. The geometries used are planar with the free stream Mach = 2.5. The compression process in inlet 2 is completely performed in external part of the inlet. Instead inlet 3 is given a mixed internal and external compression.

2. MATERIAL AND METHODS

2.1 Physical model

A mathematical model comprises equations relating the dependent and the independent variables and the relevant parameters that describe some physical phenomenon. In general, a mathematical model consists of differential equations that govern the behavior of the physical system, and the associated boundary conditions which is shown in Figure2.

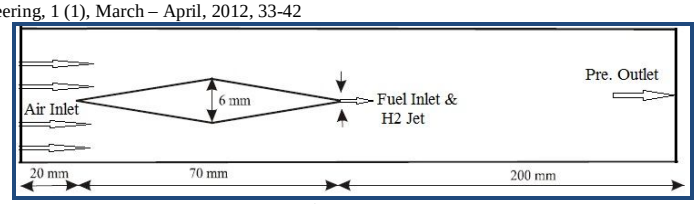

Figure 2 : Physical model of Non-premixed supersonic combustor

2.2 Governing equations

The advantage of employing the complete Navier-Stokes equations extends not only the investigations that can be carried out on a wide range of flight conditions and geometries, but also in the process the location of shock wave, as well as the physical characteristics of the shock layer, can be exactly determined. We begin by describing the three-dimensional forms of the Navier-Stokes equations below. Note that the two-dimensional forms are just simplification of the governing equations in the three dimensions by the omission of the component variables in one of the co-ordinate directions. Neglecting the presence ofbody forces and volumetric heating, the three-dimensional Navier-Stokes equations are derived as [18]:

a) Continuity equation

$$\frac{\partial \rho}{\partial t} + \frac{\partial (\rho u)}{\partial x} + \frac{\partial (\rho v)}{\partial y} + \frac{\partial (\rho w)}{\partial z} = 0 \qquad (1)$$

Where ρ is the density and u, v, w are the velocity vectors.

b) Momentum Equation In Each Direction

Applying the Newton's second law (force × acceleration) the conservation of momentum equation are given by

X-momentum equation:

$$\frac{\partial (\rho u)}{\partial t} + \frac{\partial (\rho uu)}{\partial x} + \frac{\partial (\rho vu)}{\partial y} + \frac{\partial (\rho wu)}{\partial z} = \frac{\partial \delta_{xx}}{\partial x} + \frac{\partial \tau_{yx}}{\partial y} + \frac{\partial \tau_{zx}}{\partial z} \qquad (2)$$

Y-momentum equation:

$$\frac{\partial (\rho v)}{\partial t} + \frac{\partial (\rho uv)}{\partial x} + \frac{\partial (\rho vv)}{\partial y} + \frac{\partial (\rho wv)}{\partial z} = \frac{\partial \tau_{xy}}{\partial x} + \frac{\partial \sigma_{yy}}{\partial y} + \frac{\partial \tau_{zy}}{\partial z} \qquad (3)$$

Z-momentum equation:

$$\frac{\partial (\rho w)}{\partial t} + \frac{\partial (\rho uw)}{\partial x} + \frac{\partial (\rho vw)}{\partial y} + \frac{\partial (\rho ww)}{\partial z} = \frac{\partial \tau_{xz}}{\partial x} + \frac{\partial \tau_{yz}}{\partial y} + \frac{\partial \sigma_{zz}}{\partial z} \qquad (4)$$

c) Energy equation

$$\frac{\partial (\rho E)}{\partial t} + \frac{\partial (\rho uE)}{\partial x} + \frac{\partial (\rho vE)}{\partial y} + \frac{\partial (\rho wE)}{\partial z} = \frac{\partial (u\sigma_{xx} + v\tau_{xy} + w\tau_{xz})}{\partial x}$$

$$+ \frac{\partial (u\tau_{yx} + v\sigma_{yy} + w\tau_{yz})}{\partial y} + \frac{\partial (u\tau_{zx} + v\tau_{zy} + w\sigma_{zz})}{\partial z} + \frac{\partial (k\frac{\partial T}{\partial x})}{\partial x} + \frac{\partial (k\frac{\partial T}{\partial y})}{\partial y} + \frac{\partial (k\frac{\partial T}{\partial z})}{\partial z} \qquad (5)$$

Assuming a Newtonian fluid, the normal stress σxx, σyy and σzz can be taken as combination of the pressure p and the normal viscous stress components τxx, τyy, and τzz while the remaining components are the tangential viscous stress components whereby τxy= τyx, τxz= τzx, and τyz= τzy. For

the energy conservation for supersonic flows, the specific energy, E is solved instead of the usual thermal energy H applied in sub-sonic flow problems. In three dimensions, the specific energy E is repeated below for convenience:

$$E = e + \frac{1}{2}(u^2 + v^2 + w^2) \qquad (6)$$

It is evident from above that the kinetic energy term contributes greatly to the conservation of energy because of the high velocities that can be attained for flows, where Ma>1.Equations (1)-(6) represent the form of governing equations that are adopted for compressible flows. The solution to the above governing equations nonetheless requires additional equations to close the system. First, the equation of state on the assumption of a perfect gas unemployed, that is,

$$P = \rho RT$$

Where, R is the gas constant.

Second, assuming that the air is calorically perfect, the following relation holds for the internal energy:

$$e = C_v T,$$

Where, Cv is the specific heat of constant volume. Third, if the Prandtl number is assumed constant (approximately 0.71for calorically perfect air), the thermal conductivity can be evaluated by the following:

$$k = \frac{\mu C_p}{pr}$$

The Sutherland's law is typically used to evaluate viscosity μ, which is provided by:

$$\mu = \mu o \left(\frac{T}{T_0}\right)^{1.5} \frac{T_0 + 120}{T + 120} \qquad (7)$$

Where, μ_0 and T_0 are the reference values at standard sea level conditions.

3. COMPUTATIONAL MODEL PARAMETER

3.1 Geometry and Mesh Generation

Mesh generation was performed in a Fluent pre-processing program called Gambit. The current model is diamond-shapedstrut injector with non-premixed combustion as shown in Figure 2. The boundary conditions are such that, the air inlet and fuel inlet surfaces are defined as velocity inlets and the outlet is defined as pressure outlet. Recent research has revealed that perhaps the numerical model will improve if the air inlet is defined as pressure inlet and the fuel inlet is defined as a mass flow inlet [19]. In this particular model the walls of the combustor duct do not have thicknesses. The domain is completely contained by the combustor itself; therefore there is actually no heat transfer through the walls of the combustor.

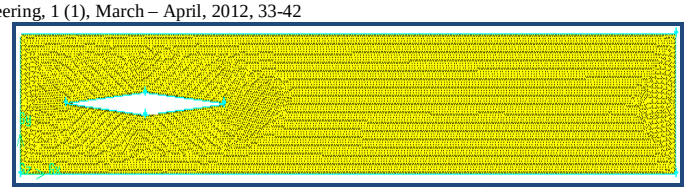

Figure 3: Two dimensional model of strut injector

3.2 Geometry and grid arrangement

The geometry of 2-D computational domain was considered for the simulation of supersonic combustion, the initial design parameters for de Laval nozzle has taken at Mach 2 which is shown in Figure 3. This was obtained by method of characteristics of nozzle program.

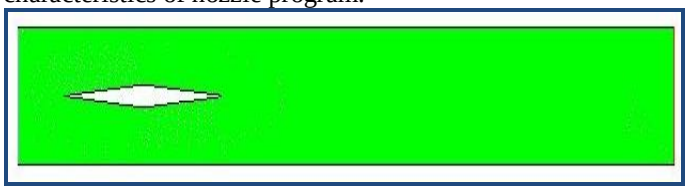

Figure 4: Grid refinement of supersonic combustor

3.3 Numerical Methodology

The model supersonic combustor considered in the present work is show in Figure 4. The combustor is 290 mm long, 36 mm at air inlet and at pressure outlet. Vitiated air enters through the inlet with hydrogen being injected through the strut injector. The Mach number at inlet is 2 and stagnation temperature and static pressure for Vitiated air are1495K and 1 bar respectively. Fuel is injected from the base which located at nozzle exit. The inlet condition of the H2 is considered as mass flow rate at 1 bar. In addition 2ddp coupled with explicit model and turbulence and finite rate chemistry are also considered.

4. BOUNDARY CONDITIONS

Table 1: Evans et al. [20] Inflow conditions of the air stream and the Hydrogen jet

Sl. No.	Free stream conditions	Oxidizer	Fuel	Fuel Stream
1.	Mach number	2	1	0.03
2.	Temperature (K)	1495	251	
3.	Pressure (bar)	1	1	
4.	Velocity(m/s)	1510	2432	
5.	Mass fraction of H_2	0	1	
6.	Mass fraction of N_2	0.425	0	
7.	Mass fraction of O_2	0.187	0	
8.	Mass fraction of H_2o	0.388	0	

4.1 Approximations and idealizations

• The gas is compressible which obeying the real gas laws and

• The flow is considered to be in steady state which is non-adiabatic.

5 RESULTS AND DISCUSSION

The results from the numerical simulation for supersonic combustion using diamond-shaped injector with non-premixed combustion model are discussed below:

5.1 Contours of total temperature

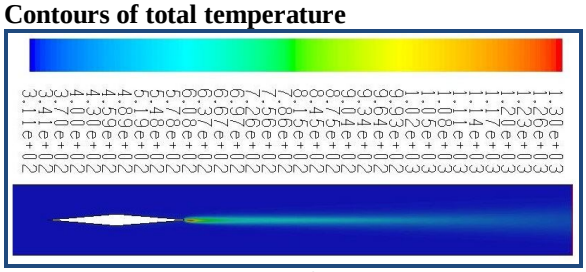

Figure 5: Contours of Total Temperature (k)

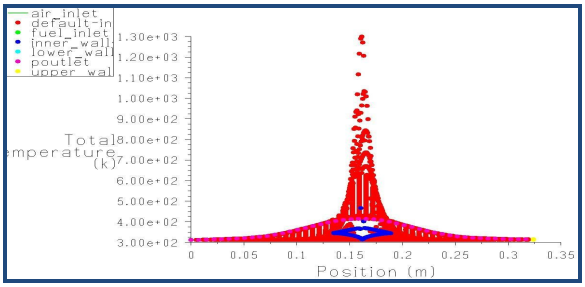

Figure 6: X-Y plot of Total Temperature

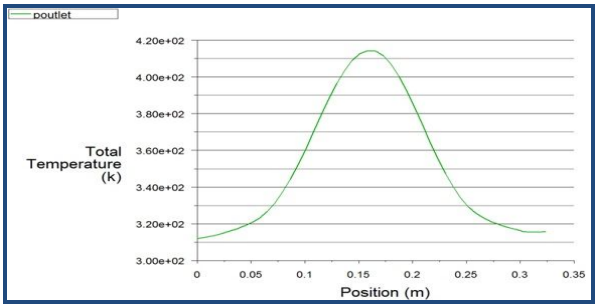

Figure 7: Total temperature distribution at pressure outlet

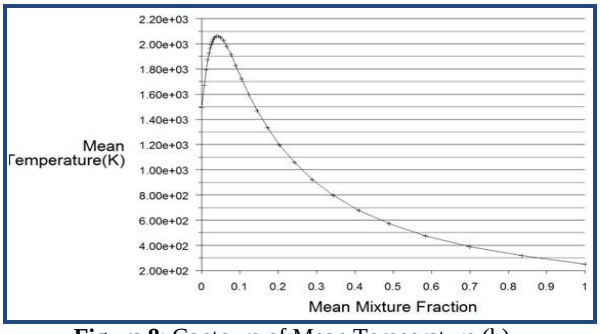

Figure 8: Contours of Mean Temperature (k)

Contour of total temperature of the resulting flow is shown in Figure 5. It is observed from the Figure 5 and Figure 6 that, the maximum temperature of 1300 k occurred in the recirculation areas which are produced due to shock wave interaction and fuel jet losses concentration and the temperature is decrease slightly a value of 311 k along the axis. The blue streamlines in the image representing the pressure gradients and hydrogen injection for the shocks. Due to combustion, the recirculation region behind the wedge becomes larger as compared to mixing case which acts as a flame holder for the hydrogen diffusion flame. The leading edge shock reflected off the upper and lower combustor walls makes the setting of combustion when it hits the wake in a region where large portions of the injected fuel have been mixed up with the air. The recompression shocks at the upper and lower corners become much weaker than mixing case. The shear layers at the base of the wedge becomes more pronounced with combustion due to the fact that continuous ignition occurs within these shear layers. The Figure 6 shows that the profile between the total temperature and the position of the combustion on all conditions such as air inlet, fuel inlet, pressure outlet, default interior and all walls whereas the Figure 7 shows that the profile between the total temperature and the position of the combustion at pressure outlet.

5.2 Contours of static temperature

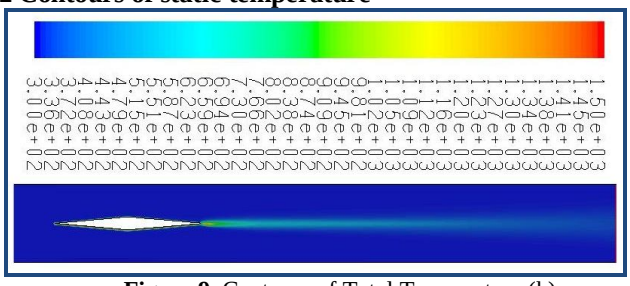

Figure 9: Contours of Total Temperature (k)

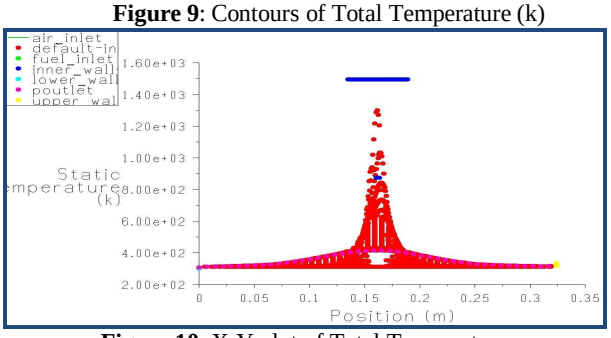

Figure 10: X-Y plot of Total Temperature

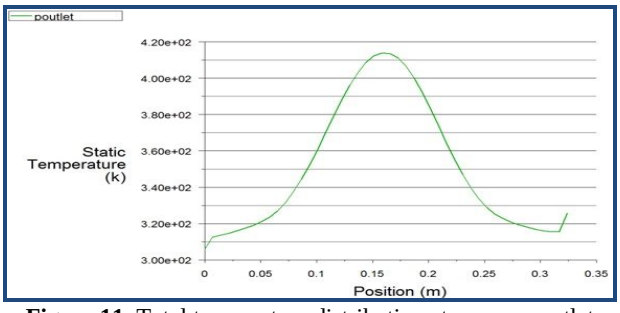

Figure 11: Total temperature distribution at pressure outlet

Contour of static temperature of the resulting flow is shown in Figure 9. It is observed from the Figure 9 and Figure 10 that, the maximum temperature of 1495 k occurred in the recirculation areas which are produced due to shock wave interaction and fuel jet losses concentration and the

temperature is decrease slightly a value of 300 k along the axis. The blue streamlines in the image representing the pressure gradients and hydrogen injection for the shocks. The Figure 10 shows that the profile between the total temperature and the position of the combustion on all conditions such as air inlet, fuel inlet, pressure outlet, default interior and all walls whereas the Figure 11 shows that the profile between the total temperature and the position of the combustion at pressure outlet.

5.3 Contours of velocity

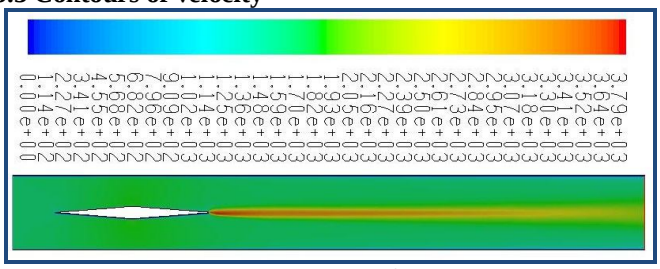

Figure 12: Contours of velocity (m/s)

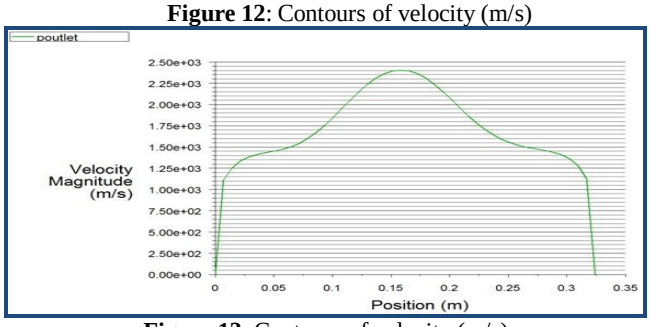

Figure 13: Contours of velocity (m/s)

The contour of velocity magnitude is shown in Figure 12. It is observed from the Figure 12 and Figure 13 that, the maximum velocity of 3788 m/s occurred in the recirculation areas. The Figure 13 shows that the profile between the total velocity magnitude and the position of the combustion at pressure outlet.

5.4 Contours of mass fraction of H2

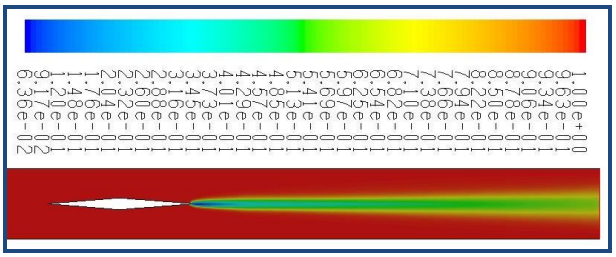

Figure 14: Contours of Mass fraction of H2

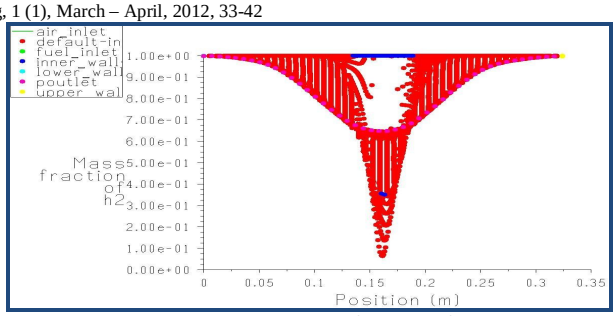

Figure 15: X-Y Mass fraction of H_2

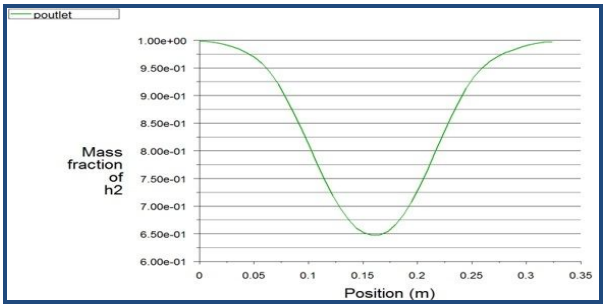

Figure 16: Contours of Mass fraction of H2

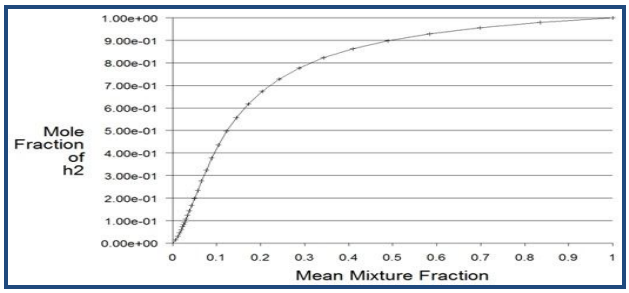

Figure 17: Contours of Mole Fraction of H2

The contour of H_2 Mass fraction plot for the flow field downstream of the injector is shown in the Figure 14. Low-velocity regions could be identified along the path of progress of the hydrogen jet. Alternate compression and expansion took place for the jet and was not enough to disorder the flow field much in the region near to the jet outlets. But the shock wave or expansion wave reflections interfered with the upcoming jet and localized low velocity regions were produced. Though, these regions are responsible for pressure loss of the jet, certainly enhanced the mixing and reaction. Lip height plays an important role in mixing enhancement. Figure 15 shows that the profile between the Mass fraction of H_2 and the position of the combustion on all conditions such as air inlet, fuel inlet, pressure outlet, default interior and all walls and the Figure 16 shows that the profile between mass fraction and the position of the combustion of H2 at pressure outlet only whereas the Figure 17 shows the mole fraction of H2.

5.5 Contours of mass fraction of N2

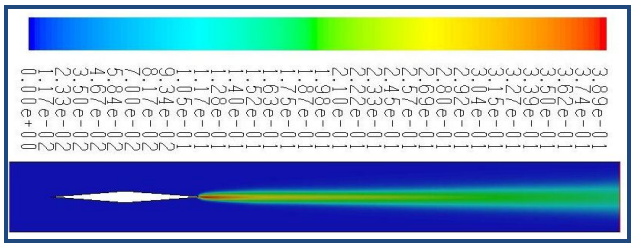

Figure 18: Contours of Mass fraction of N2

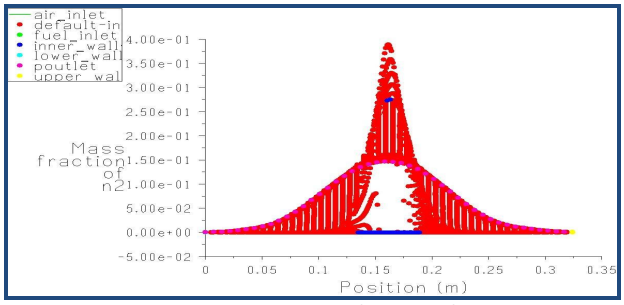

Figure 19: X-Y Mass fraction of N_2

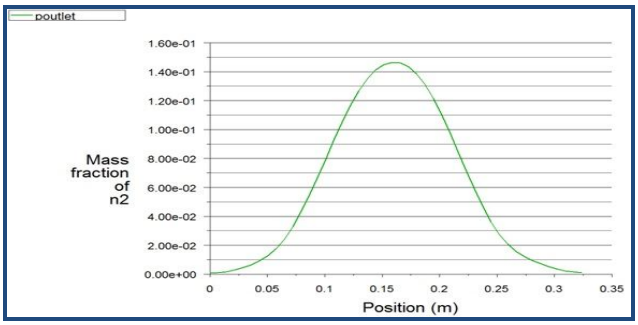

Figure 20: Contours of Mass fraction of N2 for pressure outlet

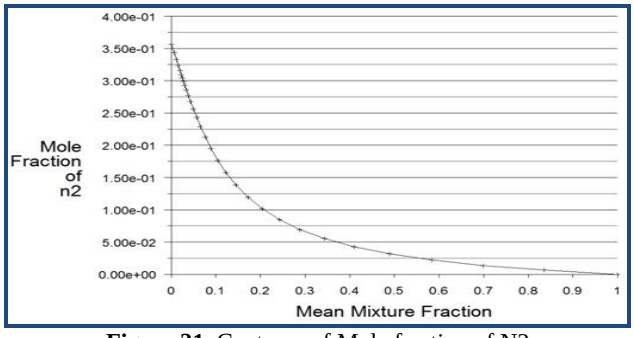

Figure 21: Contours of Mole fraction of N2

The contour of N_2 Mass fraction for the flow field downstream of the injector is shown in the Figure 21. The major ratio of the N_2 to the O_2 is 3.76. When air supplies the O_2 in a combustion reaction, therefore every mole of O_2 is accompanied by 3.76 moles of N_2. From the Figure 18 it is observed that, the maximum mass fraction of N_2 is 0.389 which is found out after combustion. Figure 19 shows that the profile between the Mass fraction of N_2 and the position of the combustion on all conditions such as air inlet, fuel inlet, pressure outlet, default interior and all walls and the Figure 20 shows that the profile between mass fraction and the position of the combustion of N2 at pressure outlet only whereas the Figure 21 shows the mole fraction of N2.

5.6 Contours of mass fraction of H2O

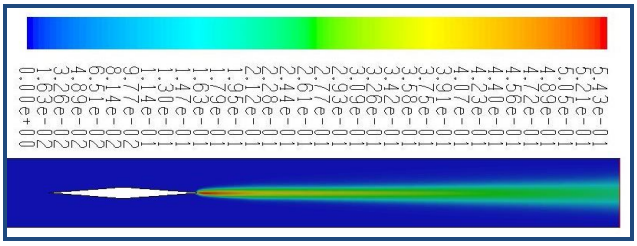

Figure 22: Contours of Mass fraction ofH O_2

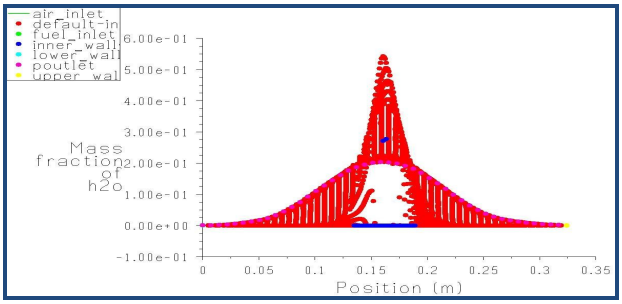

Figure 23: X-Y Mass fraction of H_2O

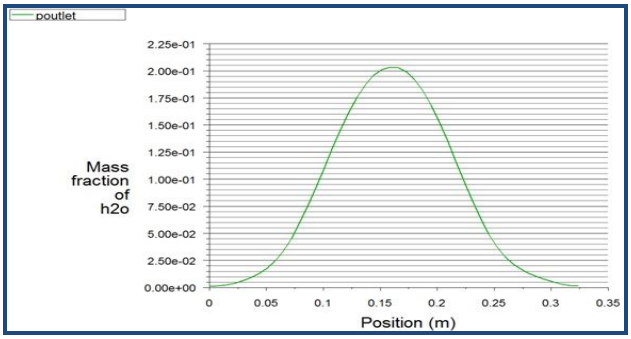

Figure 24: X-Y Mass fraction of H_2O

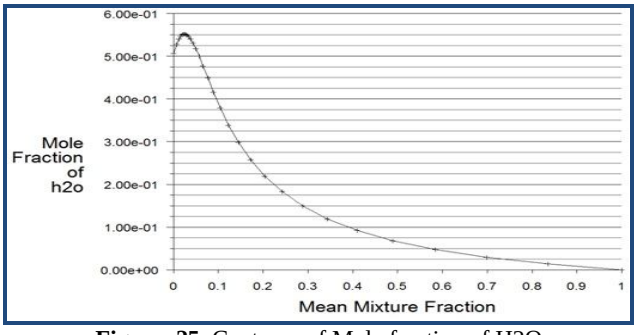

Figure 25: Contours of Mole fraction of H2O

The contour of water Mass fraction for the flow field downstream of the injector is shown in the Figure 29. From the Figure 22 is observed that, water concentration is found to be maximum value of 0.542 in the shear layer formed between the two streams of flow and the low-velocity recirculation regions within the core of the upcoming jet. Typically, when dealing the chemical reaction, it's important to remember that mass is conserved, so the mass of product is same as the mass of

reactance. Even though the element exists in different the total mass of each chemical element must be same on the both side of equation. Figure 23 shows that the profile between the Mass fraction of H_2O and the position of the combustion on all conditions such as air inlet, fuel inlet, pressure outlet, default interior and all walls and the Figure 24 shows that the profile between mass fraction and the position of the combustion of H2O at pressure outlet only whereas the Figure 25 shows the mole fraction of H2O.

5.7 Contours of mass fraction of H2O2

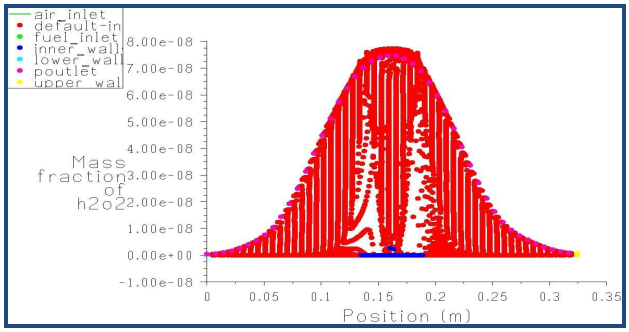

Figure 26: X-Y Mass fraction of H_2O2

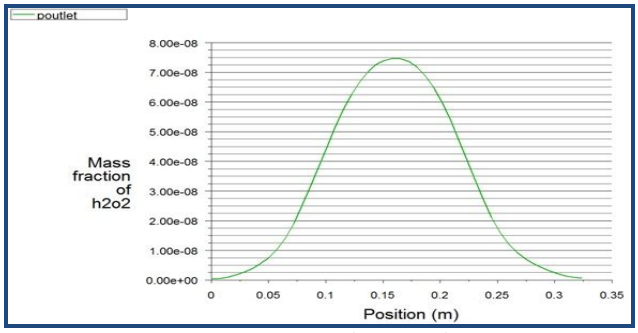

Figure 27: X-Y Mass fraction of H_2O2

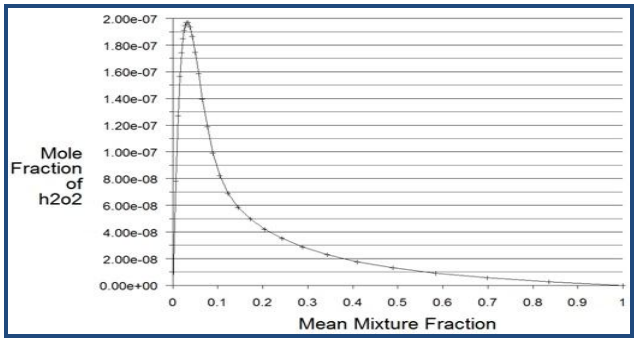

Figure 28: Contours of Mole fraction of H2O

The contour of mass fraction of H_2O_2 is shown in Figure 26. From the Figure 33 it is observed that, the maximum mass fraction of H_2O_2 is 7.74e-08 which is found out after combustion, where the minimum value is 0. Figure 26 shows that the profile between the Mass fraction of H_2O2 and the position of the combustion on all conditions such as air inlet, fuel inlet, pressure outlet, default interior and all walls and the Figure 27 shows that the profile between mass fraction and the position of the combustion of H2O2 at pressure outlet only whereas the Figure 28 shows the mole fraction of H2O2.

5.8 Contours of mass fraction of OH

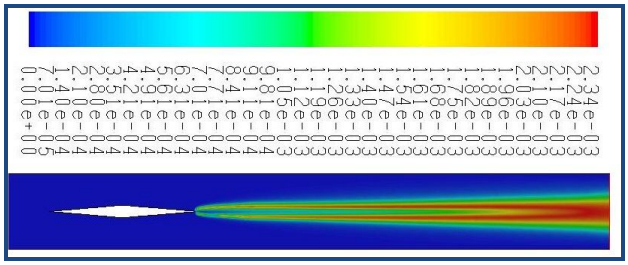

Figure 29: Contours of Mass fraction of OH

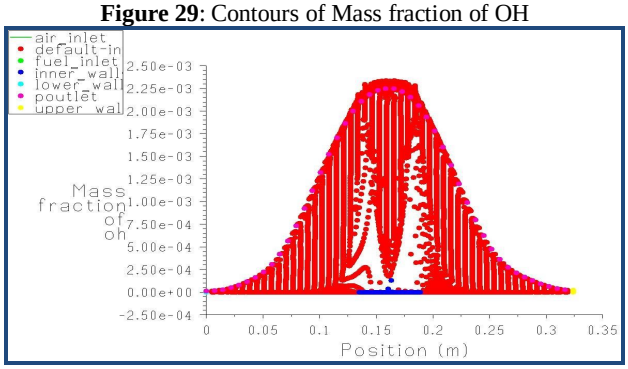

Figure 30: X-Y Mass fraction of OH

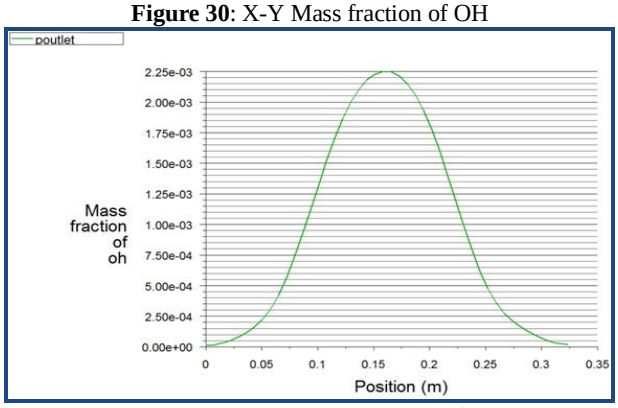

Figure 31: X-Y Mass fraction of OH

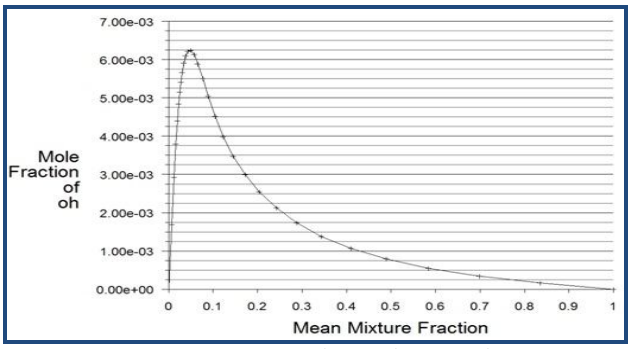

Figure 32: Contours of Mole fraction of OH

The contour of mass fraction of OH is shown in Figure 29. From the Figure 29 it is observed that, the maximum mass fraction of OH is 0.0024 which is found out after combustion, where the minimum value is 0. Figure 30 shows that the profile between the Mass fraction of OH and the position of the combustion on all conditions such as air inlet, fuel inlet, pressure outlet, default interior and all walls and the Figure 31

shows that the profile between mass fraction and the position of the combustion of OH at pressure outlet only whereas the Figure 32 shows the mole fraction of OH.

The grid independent test is shown below:

Grid size	(original /	adapted /	change)
Cells	(36540 /	119301 /	82761)
Faces	(55306 /	181241 /	125935)
Nodes	(18766 /	61940 /	43174)

6 CONCLUSION

The standard k-ε turbulence model is a simple two-equation model which is stable and numerically robust. It provides considerably accurate solutions for turbulent flow only. It can't take into account the laminar flow regions for study. The maximum temperature reached in the k-ε model is 1495K and the mass fraction of H2O is 84.2%. The occurrence of high turbulent intensity represents a high air-fuel mixing.

The high value of mass fraction of OH formed with the standard k-ε turbulence model indicates an efficient combustion process. The maximum value of mass fraction of water formed is 0.00233 which indicates nearly complete combustion of the air-fuel mixture in the zones where it is formed.

The sudden rise in density observed near the tip of the fuel injector indicates the generation of shocks which help in superior air-fuel mixing. Superior of air-fuel mixing, resulting in better quality of combustion and thus better performance.

REFERENCES

1. Heiser, W.H. and Pratt, D.T. **Hypersonic Airbreathing Propulsion**, AIAA Educational Series, 1994.
2. K.M.Pandey and T.Sivasakthivel. **CFD Analysis of Scramjet Combustor Using Strut with Circular and Planer Injector**, Proceedings of the ASME 2011 International Mechanical Engineering Congress & Exposition. IMECE2011, November 11-17, 2011, Denver, Colorado, USA, IMECE2011-62310, pp 1-9.
3. K.M.Pandey, Senior Member, IACSIT and T.Sivasakthivel. **CFD Analysis of Mixing and Combustion of a Hydrogen Fueled Scramjet Combustor with a Strut Injector by Using Fluent Software**, IACSIT International Journal of Engineering and Technology, Vol. 3, No. 5, October 2011.
4. K.M. Pandey, S.K. Reddy K.K. **Numerical Simulation of Wall Injection with Cavity in Supersonic Flows of Scramjet Combustion**, International Journal of Soft Computing and Engineering (IJSCE) ISSN: 2231-2307, Volume-2, Issue-1, March 2012, pp 142-150.
5. Eklund, D. R., Stouffer, S. D. and Northam, G. B. **Study of a Supersonic Combustor Employing Swept Ramp Fuel Injectors**, Journal of Propulsion and Power, Vol. 13, No. 6, 1997, pp. 697-704
6. Riggins, D. W. and P. H. **Vortex Generation and Mixing in Three-Dimensional Supersonic Combustors**, Journal of Propulsion and Power, Vol. 1 1. No. 3.1995, pp. 419426.
7. J. Schumacher. **Numerical Simulation of Cantilevered Ramp Injector Flow Fields for Hypervclocity Fuel-Air Mixing Enhancement,** 2000. Ph.D. Thesis, University of Toronto
8. Dudebout, R., Sislian, J. P., and Oppitz. R. **Numerical Simulation of Hypersonic Shock Induced Combustion Ramjets,** Journal of Propulsion and Power, Vol. 14, No. 6, pp. 869-879, 1998.
9. In-Seuck Jeung and Jeong-Yeol Choi. **Numerical Simulation of Supersonic Combustion for Hypersonic Propulsion**, 5th Asia-Pacific Conference on Combustion,The University of Adelaide, Adelaide, Australia 18-20, July 2005.
10. Kyung Moo Kim, Seung Wook Baek and Cho Young Han. **Numerical study on supersonic combustion with cavity-based fuel injection**, International Journal of Heat and Mass Transfer 47 , pp. 271–286, 2004.
11. Tarun Mathur. **Supersonic Combustion Experiments with a Cavity-Based Fuel Injector**, Journal of Propulsion and Power Vol. 17, No. 6, November–December 2001.
12. J. Philip Drummond, Glenn S. Diskin, and Andrew D. Cutler. **Fuel-Air Mixing And Combustion In Scramjets**, American Institute of Astronautics and Aeronautics (AIAA-.2002-3878).
13. Yves Burtschell, GhislainTchuenb and David E. Zeitoun. **H2 injection and combustion in a Mach 5 air inlet through a ViscousMach Interaction**, European Journal of Mechanics B/Fluids 29), pp.351-356, 2010.
14. D. Haworth, B. Cuenot, T. Poinsot, and R. Blint **Numerical simulation of turbulentpropane-air combustion with non-homogeneous reactants: initial results**, Center for Turbulence Research Proceedings of the Summer Program , pp.5-24, 1998.
15. YiguangJu and Takashi Niioka. **Ignition Simulation of Methane/Hydrogen Mixtures in a Supersonic Mixing Layer**, Combustionand Flame 102:462-470, 1995
16. Nitin K. Gupta, Basant K. Gupta, Narayan Ananthkrishnan_Gopal R. Shevare,IkSoo Park and Hyun Gull Yoon. **Integrated Modeling and Simulation of an Air-breathing Combustion System Dynamics**, American Institute of Aeronautics and Astronautics, pp.1-31.
17. M. Akbarzadeh and M. J. Kermani. **Numerical Computation of Supersonic-Subsonic Ramjet Inlets; a Design Procedure**, 15th. Annual

(International) Conference on Mechanical Engineering-ISME2007 May 15-17, 2007, Amirkabir University of Technology, Tehran, Iran ISME2007-3056.

18. Jiyun tu, guan Heng yeoh and chaoqun liu. **Computational Fluid Dynamics**", Elsevier Inc. 2008.
19. **Fluent**, Software Training Guide TRN-00-002.
20. Evans, J. S., Shexnayder Jr., C. J., and Beach Jr., H. L. Application of a Two-Dimensional Parabolic Computer Program to Prediction of Turbulent Reacting Flows. NASA Technical Paper 1169, 1978.

Dr. K.M.Pandey (Member IACSIT) did his B.Tech in 1980 from BHUIT Varanasi, India in 1980.He obtained M.Tech. in heat power in 1987 .He received PhD in Mechanical Engineering in 1994 from IIT Kanpur. He has published and presented more than 200 papers in International & National Conferences and Journals. Currently he is working as Professor of the Mechanical .Engineering Department, National Institute of Technology, Silchar, Assam, India. He also served the department in the capacity of head from July 07 to 13 July 2010. He has also worked as faculty consultant in Colombo Plan Staff College, Manila, Philippines as seconded faculty from Government of India. His research interest areas are the following; Combustion, High Speed Flows, Technical Education, Fuzzy Logic and Neural Networks , Heat Transfer, Internal Combustion Engines, Human Resource Management, Gas Dynamics and Numerical Simulations in CFD area from Commercial Software˝s. Currently he is also working as Dean, Faculty Welfare at NIT Silchar, Assam, India. Email:kmpandey2001@yahoo.com.

Mr. Sukanta Roga doing his M.Tech in Thermal Engineering under Mechanical Engineering Department from NIT Silchar, Assam, India from 2010. His research interest areas are CFD, Fuzzy Logic Approach, Combustion and Gasification.
Email: sukanta.me42@gmailcom.

Mr. Aditya Pratap Singh did his M.Tech in Thermal Engineering in 2008 from NIT Silchar. He has submitted his Ph.D Thesis in Department of Mechanical Engineering, National Institute of Technology, Silchar, Assam, India. His research interest areas are the following; Gas Dynamics, Combustion, High Speed Flows, Numerical Methods in Fluid Flow and Heat Transfer. Email:hello2apsingh@gmail.com